Journal of

NANOSTRUCTURES

JNS
NANOSTRUCTURES
JNS.kashanu.ac.ir

Preparation and Application of MnO$_2$ Nanoparticles/Zeolite AgY Composite Catalyst by Confined Space Synthesis (CSS) Method for the Desulfurization and Elimination of SP and OPP

M. Sadeghi [a] [*], M. H. Hosseini [a,b]

[a] *Department of Chemistry, Faculty of Sciences, Imam Hossein University, Tehran, Iran*
[b] *Nano Center Research, Imam Hossein University, Tehran, Iran*

*Corresponding author:
E-mail address*:*
meysamsadeghi45@yahoo.com
Phone: 98 9375117746
Fax: +98 2177104930

Abstract

In this work, zeolite NaY was prepared by hydrothermal method. Then, silver ions were replaced in the zeolite NaY with silver nitrate (AgNO$_3$) solution via using ion exchange (IE) method. The Manganese dioxide (MnO$_2$) nanoparticles (9.3 and 15.8 wt %) for guest were deposited in the zeolite AgY(host) structure with Mn(NO$_3$)$_2$ aqueous and KMnO$_4$ solutions by confined space synthesis (CSS) method. Synthesized samples were studied and characterized via XRD, SEM/EDAX, FTIR, AAS and N$_2$-BET techniques. The desulfurization and elimination reaction of 2-chloroethyl phenyl sulfide (2-CEPS) and DEPPT (O, S-diethyl phenyl phosphonothioate) have been investigated by 15.8 wt% Nano MnO$_2$/Zeolite AgY composite and MnO$_2$ nanoparticles catalysts and via GC, GC-MS and ^{31}PNMR.

1. Introduction

The 2-chloroethyl phenyl sulfide (2-CEPS) and O, S-diethyl phenyl phosphonothioate (DEPPT) are for the class of compounds containing sulfurous and phosphonate esters with the highly toxic that used such as pesticides, respectively [1]. The different methods are for desulfurization and elimination of these compounds. A number of oxidant contains per oxygen, sodium per borate,

hydrogen peroxide were examined as active components along with surfactants in micro emulsions for removal of pesticides [1-3]. Certain disadvantages exist with the use of these adsorbents such as environmental contaminates. [4]. In another study done via Wagner and Bartram commercially available NaY and AgY zeolites were used to investigated the reactivity of the actual pesticides [1]. Zeolites are crystalline

aluminosilicates containing pores and channels of molecular dimensions that are widely used in industry as ion exchange resins, molecular sieves, sorbents and catalysts. Zeolite Y exhibits the FAU (faujasite) structure. [5, 6]. This zeolite has a void volume fraction of 0.48, with different framework Si/Al ratios between 1.5 Si/Al 3. It thermally decomposes a 793ºC (Fig. 1). The general formulation composition of a zeolite Y is Na_2O $.Al_2O_3.4, 8 SiO_2.8, 9 H_2O$ [7-9].
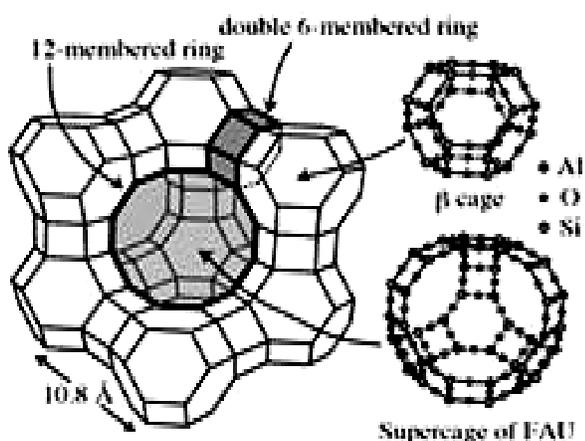
Fig. 1. Structure of crystalline zeolite Y molecular sieve (faujasite).

Manganese dioxide (MnO_2) has various applications in the elimination of pesticides. Mn is multivalent, and thus forms oxides of several different stoichiometries. For MnO_2 phases, the oxidation state is Mn^{4+}. The equilibrium phase of MnO_2 at standard temperature and pressure is -MnO_2 or pyrolusite [8], with the rutile structure, but several metastable phases are also known [10]. The purpose of this research is to use novel reactions of desulfurization and elimination of 2-chloroethyl phenyl sulfide (2-CEPS) and O, S-diethyl phenyl phosphonothioate (DEPPT) on the surface of nano MnO_2/Zeolite AgY and MnO_2 nanoparticles (NPs).

2. Experimental

2. 1. Materials

Sodium hydroxide, alumimium trihydrate, sodium silicate, $AgNO_3$, $Mn(NO_3)_2.6H_2O$ from Loba chemie Co.(India), $KMnO_4$, n-heptane, Loba chemie Co.(India), $KMnO_4$, n-heptane, methanol, n-octane phosphoric acid and $CDCl_3$ are purchased from Merck Co.(Germany). 2-CEPS (2-chloroethyl phenyl sulfide) and DEPPT (O, S-diethyl phenyl phosphonothioate) form Alfa Aesar German Fluka, were used as received.

2. 2. Physical characterization of samples

The synthesized zeolites NaY, AgY, nano MnO_2/Zeolite AgY composites and MnO_2 nanoparticles (NPs) were characterized by several different techniques, including X-ray diffraction (XRD), Scanning Electron Microscopy Energy and Dispersive X-ray Spectroscopy (SEM/EDAX, LEO-1530VP), Fourier Transform Infrared Spectroscopy (FT-IR) and Atomic absorption spectroscopy (AAS). Nitrogen Adsorption Isotherm was obtained on a quantachrome nova 1200 multipoint BET apparatus using approximately 0.1 g of sample for measurement. Immediately prior to the N_2 adsorption sample was vacuum degassed at 100 for 1h. The powder XRD patterns of catalysts were obtained using XRD measurement on a Philips diffractometer with Cu Target Kα-ray (40 kV, 40 mA and λ=0.15418 nm. The analyses were conducted at 2 theta values of 4–90º and scanned at 2°/min. The particle size and morphology of the crystalline zeolites and composite were analyzed using SEM image. For SEM, first, the samples surfaces in the presence argon plasma were covered via thin layer of Au. The observations were made at different magnifications using a Leica Cambridge S-360 SEM and JEOL scanning electron microscope.

Then, the samples photographs under vacuum were prepared. The IR spectrum was scanned using a Perkin-Elmer FTIR (Model 2000) in the wavelength range of 450 to 4000 cm^{-1} with KBr pellets method. The sample was first degassed. The NMR (Bruker 250 MHz) instrument was used for the investigation of purity 2-CEPS. Procedure for chemical analysis by AAS: 0.245 g of our synthesized samples added in a platinum crucible. This crucible was the placed in an oven at 800 ºC for a period of 2 hours. It was then cooled and reweighted to obtain the dry weight. 0.9 g of fusion mixture (potassium carbonate and lithium tetra borate in a ratio 2:1) was added to the composite materials, mixed and ashed in the furnace for another 2 hours at 800 ºC. This helps complete the decomposition of the samples. The resulting mixture was transferred to a 150 ml beaker and digested with a strong mineral acid mixture of 4 ml of HCl (12M) and 10 ml of H_2SO_4 (10%) solution. The beaker was covered with a watch glass to avoid any sample loss. The mixture was then heated on a hot plate for 30 minutes, then 4 ml of 30% hydrogen peroxide was added and the dissolution mixture was further digested for a few minutes until Effervescence stopped. The final mixture was heated overnight on a hot plate. Then, the solution was cooled and was transferred to a 100 ml volumetric flask and it was diluted to the mark with distilled water. Appropriated diluted solutions were prepared from this stock solution.

2. 3. Preparation of crystalline zeolite NaY molecular sieve by hydrothermal method

10 g of sodium hydroxide was mixed with 10 g distilled water until being dissolved. 9.75 g alumimium trihydrate was dissolved in the sodium hydroxide solution which was previously heated to 100 ºC. 10 g of the prepared solution was mixed with 61.2 g distilled water and 5.9 g of sodium hydroxide until being dissolved (solution A). The solution of 22 g sodium silicate was slowly added to the solution containing 5.9 g sodium hydroxide and 61.2 g distilled water, then, were mixed until being dissolved (solution B). Solution A was slowly added to solution B and mixture was well agitated for 30 min. The solution was transferred to a stainless steel autoclave lined with PTFE (Teflon) and kept in a static air oven at 90 ºC for 8 h. The crystalline material was separated by filtration and washed with distilled water until the pH was neutral (pH = 8). Finally, the materials were dried at 100 ºC [7, 8].

2. 4. Preparation of silver ions encapsulated in zeolite NaY by ion exchange (IE) method

2 g of zeolite NaY were calcined for 4 hours while maintaining a temperature of 400 ºC. Then, the zeolite NaY calcined as above was added to 50 ml of a 0.05 and 0.1 M silver nitrate (AgNO$_3$) solution, and the mixture was stirred for 5 hours to perform ion exchanging with maintaining the temperature at 60 ºC. The ion exchange zeolites AgY was filtered and wash with deionized water. The washed zeolite AgY was dried for 16 hours while maintaining the temperature at 110 ºC. The dried zeolite AgY was added to a heating furnace and calcined for 4 hours while maintaining a temperature of 400ºC [9, 10].

2.5. Preparation of MnO$_2$ nanoparticles in the zeolite AgY by confined space synthesis (CSS) method

The incorporation of MnO$_2$ was performed by impregnation of 0.5 gram zeolite AgY into 20 ml of a 1 M Mn(NO$_3$)$_2$ aqueous solution and stirred for 4-5 h. Then, 50 ml of a 0.13 molar KMnO$_4$ solution were added under continuous stirring.

Sample was dried for overnight at 100 ºC. Finally, the product was calcined for 4 h at 500 ºC. The obtained powder is labeled 15.8 wt% nano MnO_2/Zeolite AgY composite. In other experiment, for the preparation of 9.3 wt% of MnO_2 impregnated in faujasite zeolite AgY, 20 ml of a 1 M $Mn(NO_3)_2$ aqueous solution for 1 g of zeolite. The color of the solution immediately turned to dark brown, indicating formation and precipitation of MnO_2 according to Equation (1) The MnO_2 was formed by oxidation with $KMnO_4$ [11-14]:

$$3Mn^{2+} + 2MnO_4^- + 2H_2O \rightarrow 5MnO_2 + 4H^+ \quad (1)$$

2. 6. Adsorption/Destruction of 2-CEPS with nano MnO₂/Zeolite AgY composite and MnO₂ nanoparticles (NPs) catalysts by wetness method and its Subsequent Chemistry

In the wetness method, solvent and internal standard are added at the beginning of the experiment. But in the dry method, these materials after the reaction and the time desired to be added to the reaction mixture. So, the wetness method is more suitable than dry method has been diagnosed. For the investigation of the reaction between nano MnO_2/Zeolite AgY composite or MnO_2 nanoparticles catalysts and 2-CEPS molecule, the samples were prepared according to the following method:

For each sample, 10 μL of 2-CEPS, 5 mL methanol or n-heptane for solvent, 10 μL n-octane for internal standard and 200 mg of 15.8 wt% nano MnO_2/Zeolite AgY composite or MnO_2 nanoparticles (1:40) were added to the 100 mL Erlenmeyer flask. To do a complete reaction between composite or nanoparticles and sulfurous compound, all samples were attached to a shaker and were shaked for about 2, 4, 6 and 10 h under N_2 atmosphere and in temperature room. Then, by

micropipet extracted 10 μL of solution and injected to GC set (The carrier gas was helium with a flow rate of 1 mL.min^{-1}. Injection temperature and detector temperature of 210°C, constant temperature of 60 °C for 6 min to the column, temperature of 60 °C with a gradient of 200 min/20°C and stabilize the temperature run hold at 200 °C for 13 minutes of working conditions and the temperature program(Fig. 2) are by GC set). For the identification of destruction products, the best sample (10 μL solution was extracted and injected to column) was analyzed via GC-MS instrument Varian Star 3400 CX gas chromatograph with a flam ionization detector (FID). A fused-silica capillary column DB 5 MS, 101 mic, 30 m× 0.25 mm was used.
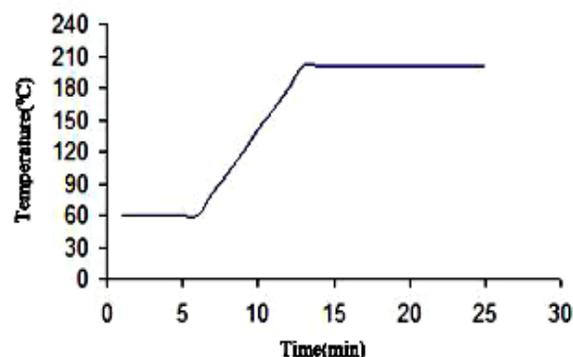

Fig. 2. The temperature program for GC set.

2. 7. Preparation of DEPPT- nano MnO₂/Zeolite AgY composite sample and its Subsequent Chemistry

To investigate the reaction nano MnO_2/Zeolite AgY composite or MnO_2 NPs and DEPPT, nano DEPPT-adsorbent sample were prepared according to the following method:

For the preparation of the phosphoric acid solution blank (0.03 M), first, 0.05 ml phosphoric acid 85% (d=1.5 g/ml) was diluted with 25 ml deionized water and injected to a capillary column and closed

two tips via heat. Then, 37 μL DEPPT, 10 ml n-heptane for solvent and 0.48 g of 15.8 wt% MnO$_2$/Zeolite AgY composite or MnO$_2$ nanoparticles (1:40) were added to the 50 mL Erlenmeyer flask and the mixture was stirred for 10 h at ambient temperature. In the next step, 1 ml solutions was Attached to centrifuge instrument (CAT.NO.1004, Universal) with 500 rpm for 5 min for do the extraction operation. Now, 0.3 ml of the up solution and 0.1 ml CDCl$_3$ were added to a NMR tube and capillary column was added to tube for the blank. At the end of, the presence of the DEPPT in the sample was investigated by the ^{31}PNMR(250 MHz Bruker) instrument. Then, by micropipette extracted 10 μL of solution and injected to GC-MS set.

3. Results and discussion

The ion exchange is performed using a sample technique where the zeolite is suspended in a aqueous solution of a soluble salt containing the desire cation at ambient temperature stirring. The ion exchange reaction, in which one type of cation is replaced with another, assumed an equilibrium state that is unique for the particular zeolite and the particular cations. Exchange between ion A^{a+}, initially in solution and ion B^{b+}, initially in zeolite may be expressed as (2):

$$bA_a^{a+} + aB_z^{b+} \leftrightarrow bA_z^{a+} + aB_a^{b+} \qquad (2)$$
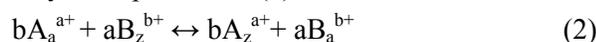
Ag^+ is the only noble monopositive cation that forms mononuclear species with appreciable stability in aqueous solution. Silver is also known to have strong influence on the absorption properties of zeolites. In the sodium zeolite NaY molecular sieve, the amounts of aluminum are low; because of its catalytic potential is decrease. Thus, ion exchange method was used to increasing the efficiency of this zeolite and the silver ions were replaced with sodium ions in zeolite NaY structure.

In the next step, manganese dioxide nanoparticles (guest) were synthesized in the pores of zeolite AgY (host) structure via using the confined space method. The reaction between manganese dioxide nanoparticles and zeolite AgY can be done three pathways (Figs. 3 and 4).
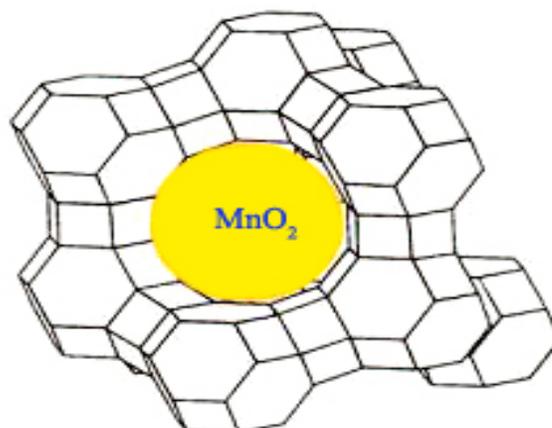
Fig. 3. The position of synthesized MnO$_2$ nanoparticle in the pore of zeolite AgY.
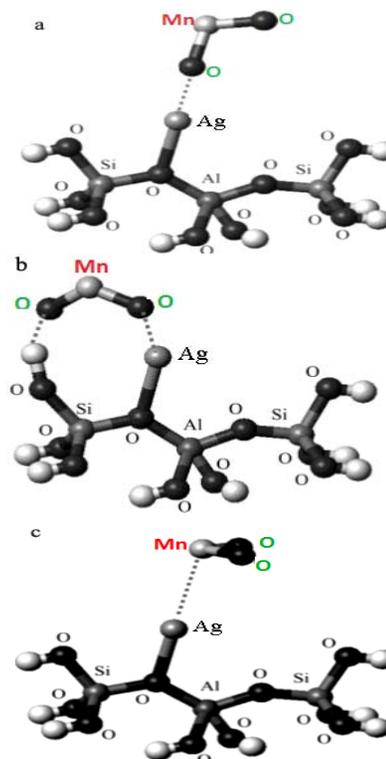
**Fig. 4.** Proposed methods of bonding between manganese dioxide nanoparticles and zeolite AgY (a)

3. 1. XRD patterns

The XRD patterns of zeolites, composites and MnO$_2$ nanoparticles are shown in Fig. 5. The structure of the zeolite NaY were retained after the silver-cation exchanges. The MnO$_2$ of 9.3 wt% deposited in the zeolites AgY does not show any new diffraction peak. Further experiments emphasized that when the loading of MnO$_2$ in the zeolite AgY, the intensity of the diffraction peak decreases, but no new peak appears. The disappearance of the XRD peaks of MnO$_2$ crystal in the sample might be explained by high dispersion of MnO$_2$ into the pores of the zeolite AgY. On the other hand, the synthesized MnO$_2$ of 15.8 wt% deposited in the zeolites AgY has a series of new peaks and revealed that MnO$_2$ nanoparticles are encapsulated into the channel of zeolite AgY. Hence, generally we can say that with silver exchange and synthesis of MnO$_2$

.

nanoparticles in the zeolite AgY, the structures of zeolites were not changed. If, weight% of MnO$_2$ are more 50 wt%, the structure of zeolite will be destructed. The structures of prepared MnO$_2$ nanoparticles encapsulated in the zeolite AgY were investigated via X-ray diffraction (XRD) measurement. The average particle size of nanoparticles was investigated from line broadening of the peak at 2θ=4-90° via using Debye-Scherrer formula (3):

$$d= 0.94\lambda/\beta\cos\theta \tag{3}$$

Where d is the crystal size, λ is wavelength of x-ray source, β is the full width at half maximum (FWHM), and θ is the Bragg diffraction angle. The average particles size by Debye-Scherrer formula was estimated to be 21 nm. Also, the average particles size was found to be 46 nm for MnO$_2$ NPs.
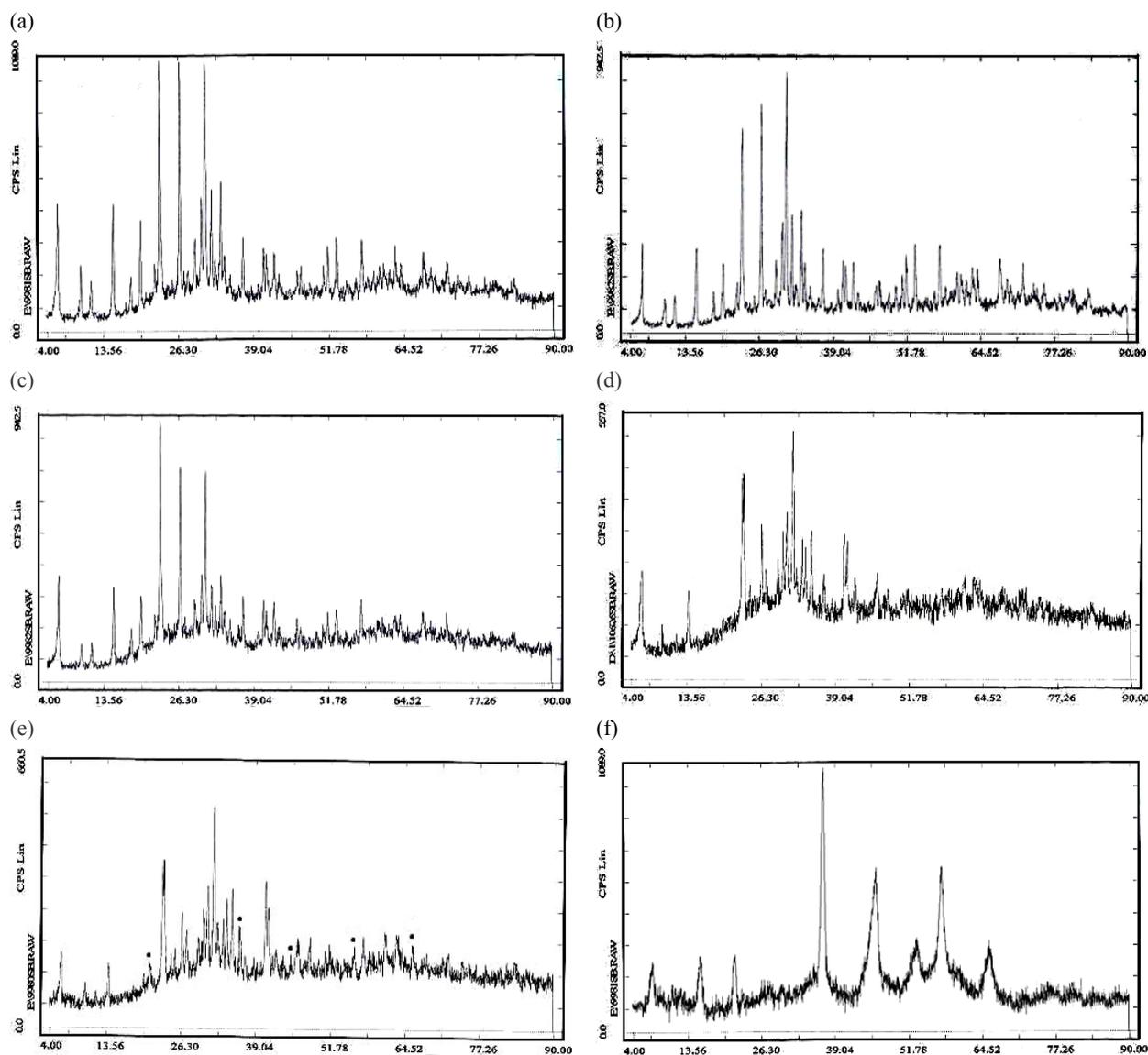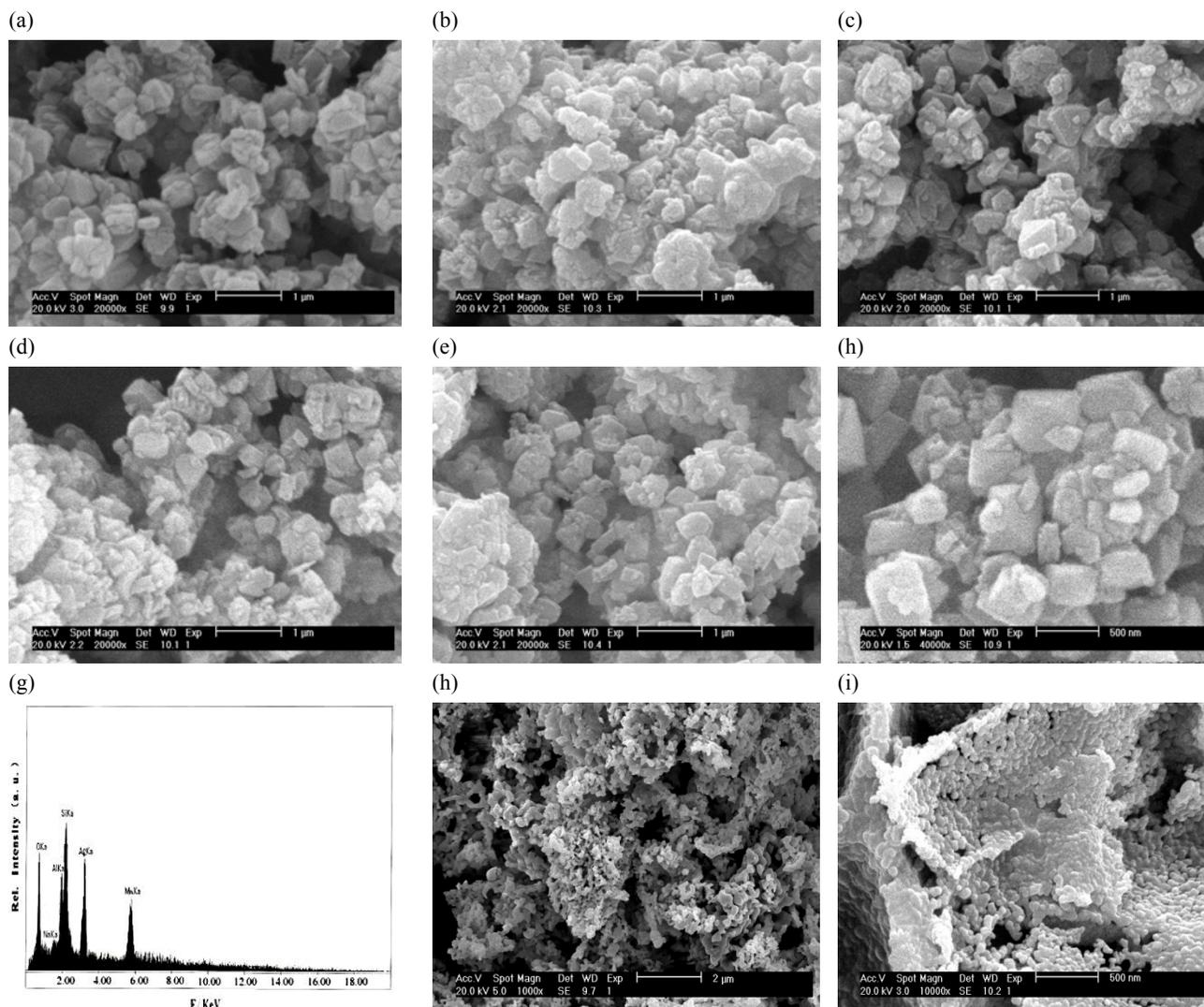
Fig. 5. XRD patterns of the samples (a) NaY, (b) AgY(1), (c) AgY(2), (d) 9.3 wt% nano MnO_2/AgY(2), (e) 15.8 wt% nano MnO_2/AgY(2) and (f) MnO_2 nanoparticles.

3. 2. SEM and EDAX studies

In Fig. 6 SEM images of samples and MnO_2 nanoparticles are given. Comparison of zeolite AgY morphology with zeolite NaY and nano MnO_2/Zeolite AgY composites shows that cubic morphology and crystallite size is retained on silver exchange and composite. For identification the composition of the synthesized 15.8 wt% nano MnO_2/AgY (2), EDAX analysis was taken. The values of silver (Ag) and manganese (Mn) elements were 22.14 wt% and 15.8 wt%, respectively.
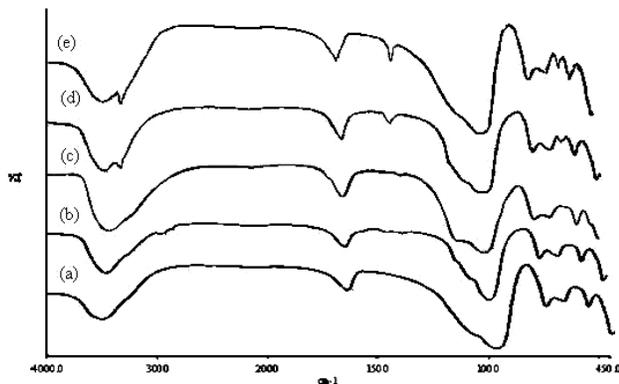
(a)

(b)

(c)

(d)

(e)

(h)

(g)

(h)

(i)

Fig. 6. SEM image of the samples (a) NaY, (b) AgY(1), (c) AgY(2), (d) 9.3 wt% nano MnO_2/AgY(2), (e) and (f) 15.8 wt% nano MnO_2/AgY(2) and (g) EDAX spectrum for 15.8 wt% nano MnO_2/AgY(2), (h) and (i) MnO_2 nanoparticles with different resolution.

3. 3. *FTIR study*

FTIR spectrum for samples is shown in Fig. 7. Peak position is nearly identical for the four samples. The peak at 466 cm^{-1} is assigned to the structure insensitive internal TO_4 (T = Si or Al) tetrahedral bending peak of zeolite Y. The peak at 566 cm^{-1} is attributed to the double ring external linkage peak assigned to zeolite Y. The peaks at 679 and 759 cm^{-1} are assigned to external linkage symmetrical stretching and internal tetrahedral symmetrical stretching respectively (D6R). Furthermore, the peaks at 980 cm^{-1} and 1080 cm^{-1} are assigned to internal tetrahedral asymmetrical stretching and external linkage asymmetrical stretching respectively and peaks around 1634 and 3479 cm^{-1} are assigned to H-O-H bending and hydroxyl groups of zeolite, respectively. FTIR spectrum of zeolites NaY and AgY are the same. But, the synthesis of nanoparticles with different amounts of Manganese dioxide (with contents of

9.3% and 15.8 %) in the pores zeolite AgY will cause new peaks (3416, 1430 and 570 cm^{-1}).

Fig. 7. FTIR spectrum of the samples (a) NaY, (b) AgY(1), (c) AgY(2), (d) 9.3 wt% nano MnO$_2$/AgY(2) and (e) 15.8 wt % nano MnO$_2$/AgY(2).

3. 4. Atomic absorption spectrometry (AAS) analysis

For the investigation the wt% of silver/manganese elements in the samples of atomic absorption spectrometry (AAS) was used. For analysis of elements for samples, five standard solutions which ranged from 10 ppm to 50 ppm were prepared. Finding the absorbance of these solutions enables us to draw standard curve, and from this curve we were able to find the concentration of solution to be analyzed, knowing their absorbance (Fig. 8).
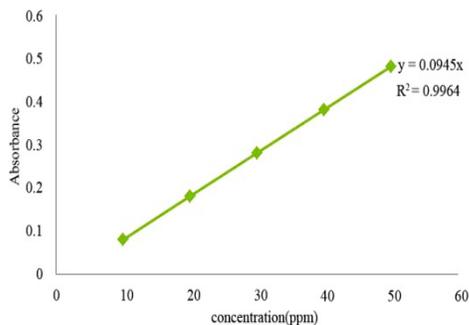
Fig. 8. Standard curve of absorbance versus concentration.

According to the standard curve by diluting the samples and the results are as follows: The %silver/ Manganese were determined using the following equation (4):

$$R_a/R_{std}(C_{std}/W_a)(V_a)(M/F)(D.F) \times 100 \qquad (4)$$

R_a: reading obtained from the sample solution, R_{std}: reading obtained from the sample standard, C_{std}: concentration of standard solution (ppm), W_a: weight of the dried sample (g). V_a: volume of original sample solution used (ml), M: molecular weight of the element in the oxide from (g/mol), F: formula weight of element (g/mol), D.F: dilution factor. We could define dilution factor using the the following equation:

$$D.F: V_{ds}/V_{ad} \qquad (2)$$

Where; V_{ds}: Volume of the dilution sample solution (ml), V_{ad}: volume of aliquot taken from the dilution (ml). Results from the standard curve are in Table 1.

Table 1. Results from the standard curve

Sample	C [ppm]	Ag [wt%]	Mn [wt%]
AgY(1)	181.47	13.52	-
MnO$_2$/AgY(2)	94.29	-	9.3

3. 5. N$_2$-BET analysis

The structure properties of samples were obtained from the nitrogen adsorption isotherm or Brunauer-Emmett-Teller (BET) and are listed in Table 2. As seen, with increasing amounts of MnO$_2$ loading in the zeolite, the BET (surface area) values were decreases. Hence, this emphasized that ratio the pores of zeolite AgY are occupied via Manganese dioxide particles.

Table 2. Properties of synthesized samples

| Sample	Total Pore volume (cm^3/g)	BET-Surface area (m^2/g)	Average pore size (nm)
NaY	0.47	424.54	1.8
AgY(1)	0.32	383.66	1.8
AgY(2)	0.29	375.11	1.8
9.3 MnO$_2$/AgY(2)	0.26	356.19	1.8
15.8 MnO$_2$/AgY(2)	0.21	335.97	1.8

3. 6. ^{1}HNMR and GC analyses

The effects solvent and time on the adsorption/destruction reaction were investigated. Without a solvent, the complete reaction can take days or weeks to do. On the other hand, with increasing of time, efficiency of elimination reaction is increased. To investigate the purity of 2-CEPS and its retention time, ^{1}HNMR and GC spectrums of this compound is taken (Figs. 9 and 10). The methanol and n-heptane solvents were indicated at retention times between 2 and 3, 6 and 7 min, respectively. The n-octane and 2- CEPS peaks are diagnosed at retention time 9 and 15.3 min. The evaluation the reaction between 15.8 wt% nano MnO$_2$/AgY(2) composite and MnO$_2$ nanoparticles catalysts with 2-CEPS molecule at ambient temperature (25±1˚C) via GC analysis shows that these compounds have a high performance for adsorption and destruction of 2-CEPS. The results of adsorption/destruction reaction for methanol were different from n-heptane. 66% of 2-CEPS was adsorbed and destructed in the contact with 15.8 wt% nano MnO$_2$/AgY(2) catalyst in the methanol solvent after 10 hours. However, in the n-heptane solvent

as similar time, 84% of 2-CEPS molecule was adsorbed and destructed for this time. On the other hand, these values for MnO$_2$ NPs are lower and were 42% and 51% in the methanol and n-heptane, respectively. The GC chromatograms for the different time and solvents and results of these chromatograms are shown in Figs. 11-13 and Table 3. As seen from the chromatograms that the peak intensity (area under curve: AUC) of 2-chloroethyl ethyl sulfide in the heptane solvent is much lower than methanol solvent. This means that the potential degradation of 2-CEPS in the non-polar n-heptane solvent is higher than the polar methanol. Hence, deduced that in the elimination reaction, we have a competition between 2-CEPS molecule and methanol solvent to be occupied active sites of adsorbents (composite and MnO$_2$ NPs) and catalyst that consequently, the adsorption reaction is reduced. On the other hand, n-heptane is an inert solvent. Due to there is any competition between it and the 2-CEPS, molecule can be easily adsorbed via adsorbents.
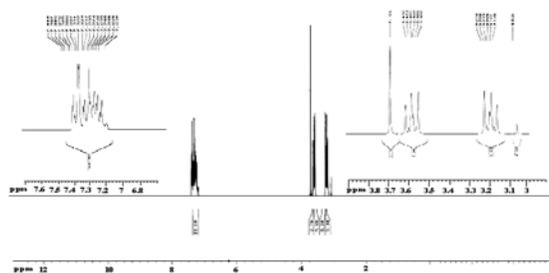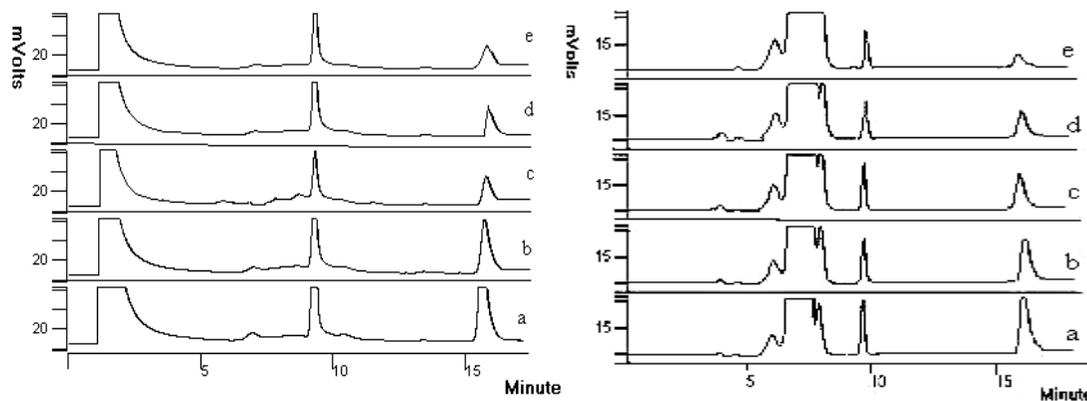
Fig.9. ^{1}HNMR spectrum of 2-CEPS.
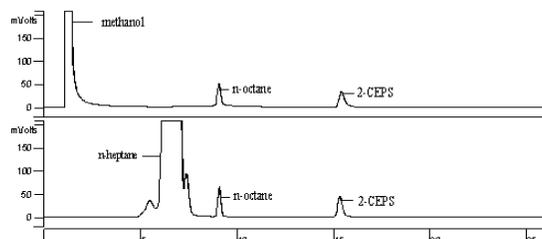
Fig.10. GC chromatograms for 2-CEPS, n-octane, methanol and n-heptane and that's retention times.
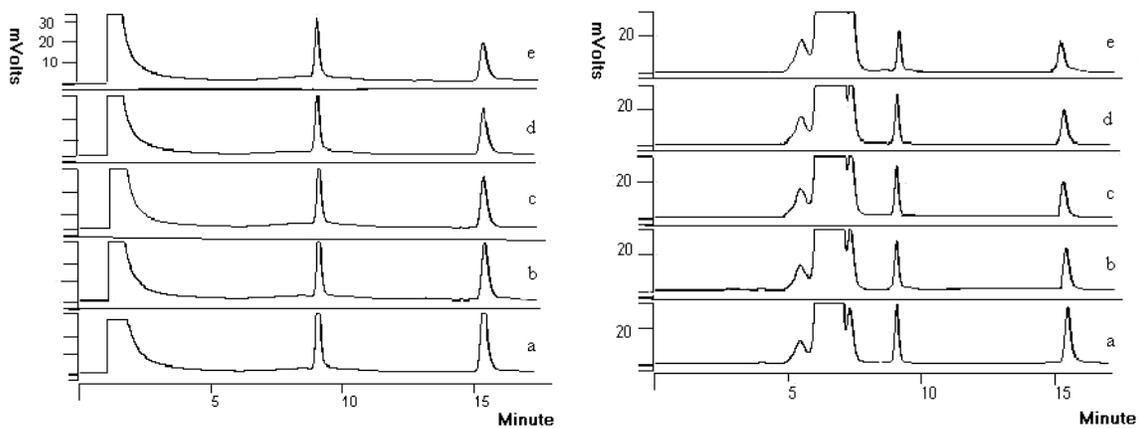
Fig.11. GC chromatograms for 2-CEPS in the presence of MnO$_2$ NPs, in (left) methanol and (right) n-heptane.

Fig. 12. GC chromatograms for 2-CEPS in the presence of 15.8 wt % nano MnO$_2$/AgY (2), in (left) methanol and (right) n-heptane.
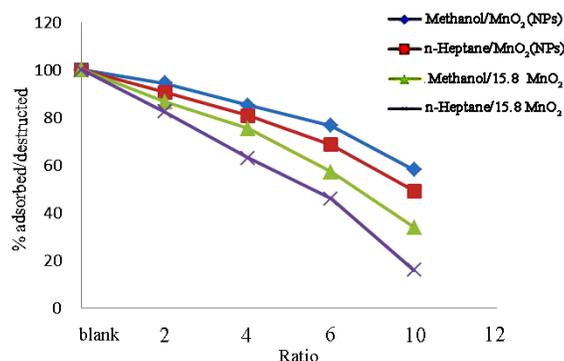
Fig. 13. The curve of %adsorbed/destructed 2-CEPS versus time.

Table 3. The results of GC analysis in the presence of different solvent and time

Sample	Time(h)	% Reduced/MnO$_2$ nanoparticles(NPs)		% Rreduced /15.8 wt% MnO$_2$/AgY(2)	
		methanol	n-heptane	methanol	n-heptane
a	Blank(0)	100	100	100	100
b	2	94.42	90.56	86.47	82.36
c	4	85.15	80.78	75. 28	62.97
d	6	76.54	68.59	57.16	45.35
e	10	58.13	49.22	33.82	15.98

3.7. GC-MS and FTIR analyses

To identify the composition of elimination product of 2-CEPS molecule with nano MnO$_2$/AgY catalyst gas chromatography coupled with mass spectrometry (GC-MS) analysis was used. In Fig. 14 Failures of the mass spectrums of 2-chloroethyl phenyl sulfide and phenyl vinyl disulfide were shown. The detector was set to scan two peaks at retention time of 15.3 and 19.7 minutes with mass range of 28 to 172 m/z and 28 to 136 m/z for 2-CEPS (remaining) and phenyl vinyl disulfide (PVS), respectively. After the reaction, the adsorption of 2-CEPS on the nano MnO$_2$/AgY composite was investigated via FTIR spectrum (Fig. 15). The new peaks in 857, 1201 and 1261 and 1372 cm^{-1} are corresponded to adsorbed 2-CEPS.
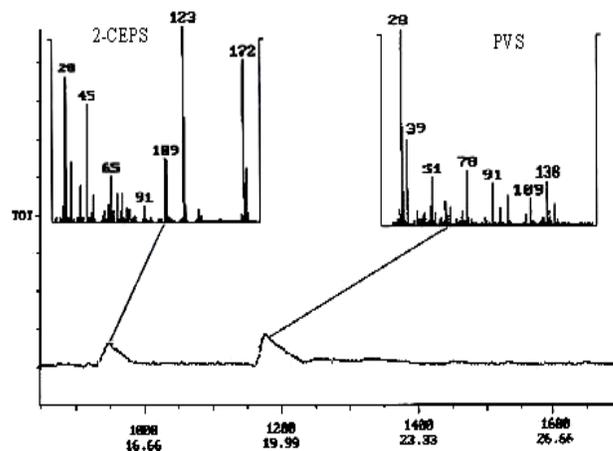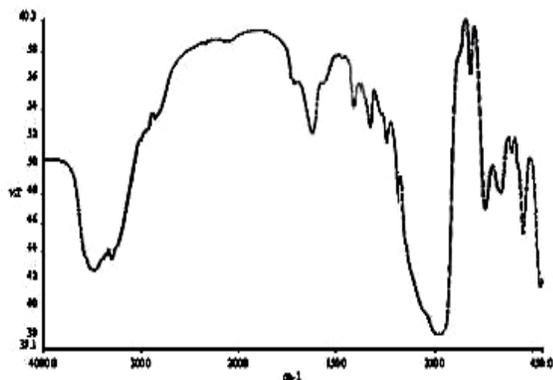

**Fig. 14.** GC-MS analysis and Failures of the mass spectrums of 2-CEPS and PVS.

Fig. 15. FTIR spectrum of the nano MnO$_2$/AgY after adsorption of the 2-CEPS.

After the identification of the destruction reaction product of 2-CEPS with nano MnO$_2$/AgY composite, its proposed mechanism (subsequent chemistry) of adsorption and destruction of this reaction will provide (Scheme 1). The reactions between the zeolite AgY and 2-chloroethyl phenyl sulfide has several sections:

Section I) Adsorption reaction with nucleophillic attack the Ag atoms of zeolite to the chlorine and sulfur atoms of 2-CEPS molecule. In this interaction, the chlorine atom in 2-chloroethyl phenyl sulfide will be removed (the dehalogenation reaction). Section II) in the present of H$_2$O molecule, via nucleophillic attack the hydroxyl group and silver cation to $^+$SCH$_2$CH$_2$Ph molecule and elimination of HCl, the cyclic of sulfur was cleavaged (the hydrolysis reaction). Section III) in the next step, from the Ag$^+$ attack to oxygen atom of hydroxyl group, H$_2$O was eliminated. On the other hand, the interactions between MnO$_2$ and 2-chloroethyl phenyl sulfide has two sections (Scheme 2):

I) Adsorption reaction with nucleophillic attack the Mn atoms and the Bronsted acid sites (OH) of MnO$_2$ to the chlorine and sulfur atoms of 2-CEPS. In this reaction, chlorine atom in 2- chloroethyl phenyl sulfide will be removed (dehalogenation

reaction). II) Destruction reaction with nucleophillic attacks the Bronsted acid sites (OH) of MnO$_2$ to the hydrogen atom of 2-CEPS. In this reaction, water will be removed (hydrolysis reaction).
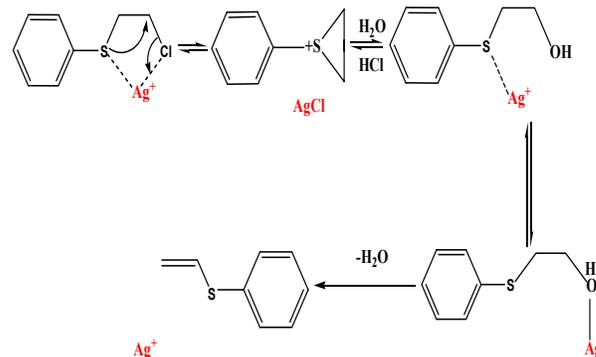
Scheme 1. Proposed reaction mechanism for adsorption and destruction of 2-CEPS on the Ag$^+$ cation of zeolite AgY.
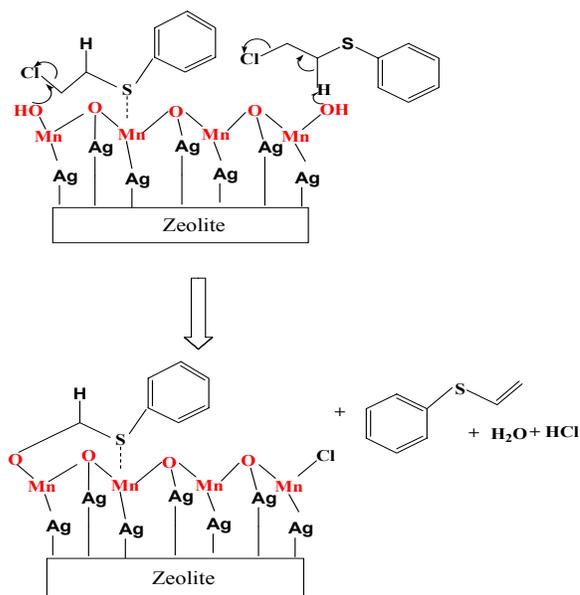

**Scheme 2.** Proposed reaction mechanism for adsorption and destruction of 2-CEPS on the MnO$_2$ nanoparticles.

3. 8. ^{31}PNMR and GC-MS analyses

^{31}PNMR spectrums for interaction between O, S-diethyl phenylphosphonothioate (DEPPT) and 15.8 wt% nano MnO$_2$/AgY(2) composite and MnO$_2$ NPs are showed in Fig. 16. The intensity of

the DEPPT peak decreases and also, a new peak appears for the destruction product. Hence, we can say that after 10 h, more 40% and 70% organophosphosphate molecule was adsorbed and destructed via MnO_2 NPs and 15.8 wt% nano MnO_2/AgY(2) respectively. The destructed major products of this reaction; i.e. ethyl phenyl phosphonic acid (EPPA) with a mass 28 to 184 m/z were identified via GC-MS analysis (Fig .17). Silver ethylmercaptide (AgEt) was adsorbed on the composite. For this interaction, proposed mechanism which is shown in Scheme 3. The DEPPT similarly hydrolyzes via P−S cleavage on AgY to yield an apparent silver salt of ethyl phenyl phosphonate, which does not undergo further reaction to the desulfurized analogue. The MnO_2 nanoparticles have approach and condition the same with zeolite AgY. No reaction is observed for DEPPT on the zeolite NaY(Na^+ cations).

(a)

(b)

(c)

(d)
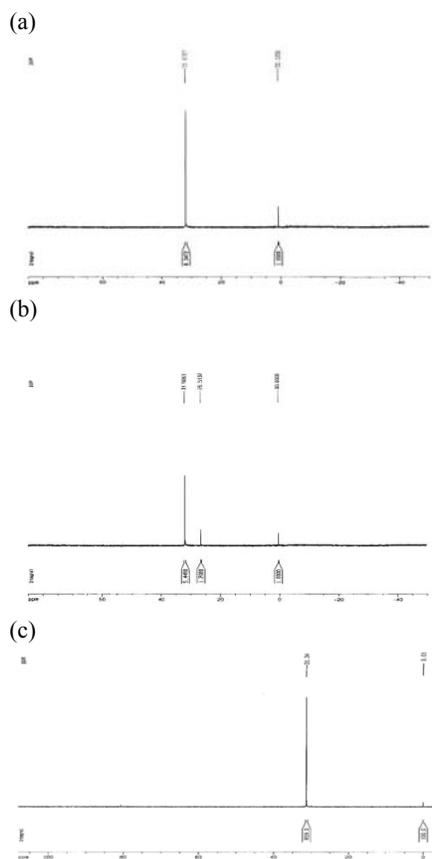
Fig. 16. ^{31}PNMR spectrums of the adsorption/destruction of DEPPT on (a) MnO_2 NPs and on (b) 15.8 wt% nano MnO_2/AgY(2), (left) blank (t=o) and (right) after t=10 h.
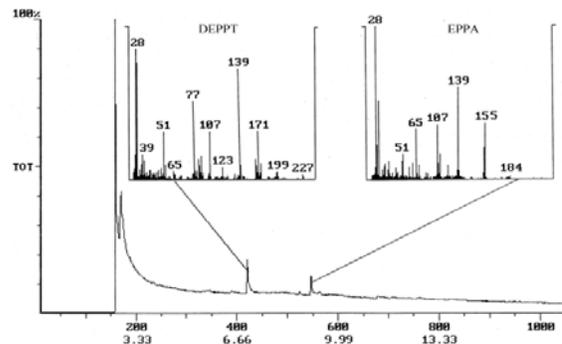
Fig. 17. GC-MS analysis and Failures of the mass spectrums for DEPPT and EPPA.

4. Conclusion

In the present study, zeolites NaY and AgY were synthesized by hydrothermal and ion–exchange (IE) methods, respectively. Then, nano MnO_2/Zeolite AgY with different contents of manganese dioxide and MnO_2 nanoparticles(NPs) were prepared via and CSS method. The ability of nano MnO_2/Zeolite AgY composite and MnO_2 nanoparticles for the adsorption and destruction of 2-CEPS molecule were investigated. In fact, with a simple and low cost method, fine particles with high performance were synthesized. Summarily, synthesized 15.8 wt% nano MnO_2/AgY(2) composite could adsorption and destruction 2-CEPS about %66 and %84 after 10 h. But, these values for MnO_2 nanoparticles are lower.
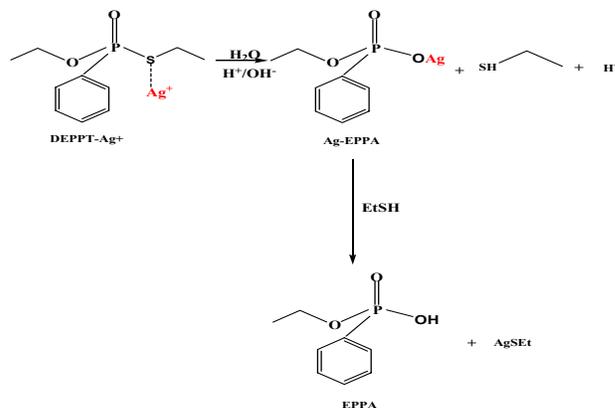
Scheme 3. Proposed reaction mechanism for adsorption/destruction of DEPPT on the nano MnO_2/AgY.

Table 4. The results of ^{31}PNMR spectrums.

Time(h)	0	10	
AUC DEPPT/AUC H_3PO_4, MnO_2 NPs	8.3472	5.449	1.200
AUC DEPPT/AUC H_3PO_4, 15.8 wt% MnO_2/AgY(2)	8.590	3.623	1.768

Destruction product (PVS) was diagnosed that has less toxic in compare to 2-CEPS. On the other hand, the reaction DEPPT molecule with MnO_2 nanoparticles and 15.8wt% nanoMnO_2/AgY(2) composite were investigated after 10 h. In this reaction, more 49% and 78% DEPPT is adsorbed and destructed. Elimination single product; i.e. ethyl phenyl phosphonic acid (EPPA) has been identified.

Acknowledgment

References

[1] P.W. Bartram, G.W. Wagner, US Patent 2003, 6,537, 382.

[2] S.C. Stout, S.C. Larsen, V. H, Micropo. Mesopor. Mater. 100 (2007) 77.

[3] S.H. Kim, US Patent, 2006, 0162557 A1.

[4] C.W. Kanyi, Micropo. Mesopor. Mater. 124 (2009) 232.

[5] C.H. Bärlocher, W.M. Meier, D.H. Olson, Rev. Ed., Elsevier, 2001.

[6] H. Ghobarkar, O. Schläf, U. Guth, Prog. Solid. St. Chem. 27(1999) 29.

[7] M. Rasouli, N. Yaghobi, S. Chitsazan, M.H. Sayyar, Micropo. Mesopor. Mater. 11 (2011) 045.

[8] C.H. Elliott, C.V. McDaniel, US Patent 1970, 3,639,099.

[9] S.O. Kim, E.D. Park, E.Y. Ko, Patent 2006, 016, 25, 57 A1.

[10] L. Ligang, Y. Zhang, Y. Hong, F. L. Zhang, Collo. Inter. Sci. 360 (2011) 753.

[11] Z.Y. Yuan, R.T. Zhen, Chem. Phys Lett, 389 (2009) 83.

[12] M. Richter, H. Berndt, R. Eckelt, M. Schneider, R. Fricke, 54 (1999) 531.

[13] B. Shen, Chinese Chem Lett, 11 (2000), 649.

[14] A. Escobedo-Morales, F. Ramirez-Vergara, Encue, Inter. Nanocie. Nanotec.